Analytical and Numerical Solutions for Nonlinear Equations
©Available online at https://ansne.du.ac.ir/
Online ISSN: 3060–785X
2026, Volume 11, Issue 1, pp. 142–152
Research article

Analytical and Numerical Bounds for a Nonlinear Overlap Model of Circular Sectors

Fereshteh Tahmasi[1], Mahmood Shakoori[1,*], Leila Nasiri[1]

[1] Department of Mathematics, Lorestan University P. O. Box 465, Khoramabad, Iran

*** Corresponding author(s):** shakoori.m@lu.ac.ir

Received: 16/02/2026 **Revised:** 30/03/2026 **Accepted:** 06/04/2026 **Published:** 07/06/2026 10.22128/ansne.2026.3249.1195

Abstract

In this paper, we investigate a nonlinear analytical model for estimating the overlap area between two circular sectors. The overlap problem is formulated in a functionalanalytic framework by representing sector regions through indicator functions and interpreting the overlap area as a nonlinear trace expression involving multiplication operators on $L^2(\mathbb{R}^2)$. This formulation allows the application of classical nonlinear inequalities, including Youngs inequality and related operator bounds, to derive explicit analytical estimates for the overlap area. The resulting bounds depend nonlinearly on the sector parameters, such as angular widths and radii, and avoid direct geometric intersection computations. In addition, the proposed bounds are numerically tractable and can be efficiently evaluated numerically for a wide range of sector configurations. An angularaveraged nonlinear bound is introduced, providing a computable upper estimate that captures the combined angular and radial effects of the sectors. Several illustrative examples demonstrate the effectiveness of the analytical bounds and confirm their numerical consistency. The proposed approach establishes a connection between nonlinear analytical techniques, operator inequalities, and geometric modeling, offering a flexible framework for nonlinear overlap estimation problems. This formulation presents an innovative conceptual reformulation using operator theory for the circular overlap problem, providing a powerful tool for analysis and accurate estimation of the overlap area using classical inequalities.

Keywords: Circular sector overlap, Geometric modeling, Operator inequalities, Analytical bounds, Computational geometry

Mathematics Subject Classification (2020): 47A63, 52A38, 26D15, 68U05, 65D18, 94A05

1 Introduction

The analysis of overlaps between circular sectors arises naturally in several mathematical and engineering contexts. While the overlap of two disks has long been studied and closed-form results are available, the presence of angular constraints in sectors makes their intersection significantly harder to describe. This difficulty becomes particularly important in applied settings: in wireless communications, sector antennas define coverage regions whose overlaps directly affect network performance; in computational geometry and robotics, sectors represent fields of view or sensing cones, where overlap detection is crucial for navigation and collision avoidance [1, 2, 6, 13, 16].

Despite these broad applications, the literature has primarily focused on complete circular intersections or approximate numerical

schemes, such as polygonal discretization or Monte Carlo methods [7,9]. These approaches provide useful estimates but do not offer general analytic characterizations when radial boundaries and angular parameters must be explicitly considered. Moreover, while measure-theoretic frameworks in integral geometry establish a strong foundation for analyzing sets and their intersections, few works have adapted these ideas specifically to circular sectors. This leaves an evident gap between geometric modeling and analytic tractability [3,12].

Definition 1. *A* circular sector *is a geometric region of the plane defined by a circle of radius $r > 0$ and two radii emanating from the circles center. Geometrically, the sector is the portion of the disk enclosed between these radii and the corresponding arc of the circle. Formally, in polar coordinates (r', φ) with respect to the circles center O, the sector can be expressed as*

$$S = \left\{ (r', \varphi) \mid 0 \le r' \le r,\ \alpha \le \varphi \le \alpha + \theta \right\},$$

where α denotes the starting direction and $\theta > 0$ is the central angle of the sector.

A circular sector is uniquely determined by three parameters:

- *the radius r, which specifies the distance from the center to the arc boundary;*
- *the central angle θ, which defines the angular aperture of the sector;*
- *the orientation α, which fixes the position of the sector in the plane.*

Two classical quantities associated with a sector are its area and the length of its arc. Since the area of a full circle is πr^2, the sectors area is proportional to the ratio $\theta/2\pi$, giving

$$A = \frac{1}{2}\theta r^2. \tag{1}$$

Similarly, the arc length is proportional to the same ratio of angles relative to the circumference $2\pi r$, which yields

$$L = r\theta.$$

These fundamental relations show that both the area and the arc length of a sector depend linearly on the central angle and grow with the radius, forming the geometric foundation for further analysis of overlaps between sectors.

The study of overlaps between geometric regions has a long history, primarily in the context of circle–circle intersections, where closed-form lens formulas are well established [2]. These results, however, are not directly transferable to sector–sector intersections because of angular boundaries and radial constraints. Research in computational geometry has introduced approximation-based methods such as polygonal decomposition and grid sampling, but such approaches prioritize numerical convenience over analytic rigor and fail to generalize across configurations [16,17].

In applied contexts, particularly in wireless communications, the modeling of antenna beam patterns as circular sectors has made overlap analysis a recurring problem. Antenna design and frequency planning often depend on the careful management of beam overlaps to optimize coverage and reduce interference [1]. Yet, much of this literature approaches overlaps empirically or via simulation, rather than providing analytic frameworks. On the analytic side, functional analysis and operator theory offer powerful tools for addressing such geometric problems. The interpretation of sector indicator functions as multiplication operators in L^2 spaces connects geometry with operator inequalities. Foundational results in operator theory establish key properties: projection operators are contractive and idempotent; multiplication operators associated with non-negative functions are positive semidefinite, ensuring that analytic bounds align with geometric intuition [4].

Furthermore, classical inequalities such as the Cauchy–Schwarz inequality [19] and Youngs inequality [10] provide rigorous bounds for overlap measures without requiring explicit case-by-case integration. Recent extensions of Youngs inequality to matrix and operator contexts strengthen this analytic foundation, while results on trace-class operators show that the trace of a multiplication operator corresponds directly to geometric measure [10,18]. These connections form the backbone of a functional-analytic approach to sector overlaps. From a mathematical viewpoint, the overlap estimation considered in this work can be formulated as a nonlinear analytical problem, since the derived bounds depend nonlinearly on the underlying geometric parameters of the sectors.

Contribution and novelty. In this work, we introduce a nonlinear analytical framework for estimating overlap quantities arising from sectorbased geometric models. The overlap area is formulated as a nonlinear trace functional involving multiplication operators on $L^2(\mathbb{R}^2)$,

which enables the systematic application of nonlinear operator inequalities. The proposed formulation leads to explicit analytical bounds that depend nonlinearly on the geometric parameters of the sectors and can be efficiently evaluated in a numerical manner, without requiring explicit computation of geometric intersection regions. In particular, an angularaveraged nonlinear bound is derived, providing a computable, symmetric, and interpretable estimate for the overlap area. Unlike classical geometric approaches that rely on casedependent constructions, the proposed framework offers a unified nonlinear analytical treatment suitable for both theoretical investigation and numerical evaluation. This formulation places the overlap estimation problem within the broader class of nonlinear analytical models governed by functional inequalities.

2 Preliminaries

This section establishes the foundational concepts and results that will be used in later developments. The relations are presented progressively: starting with measurable sets and indicator functions, then multiplication operators and projections, and finally trace properties, positivity, and classical inequalities.

We start with the most basic building block, the indicator function of a measurable sector. Let $S_i \subset \mathbb{R}^2$ be a measurable set. Its characteristic (indicator) function is defined by

$$\chi_i(x) = \begin{cases} 1, & \text{if } x \in S_i, \\ 0, & \text{otherwise}, \end{cases} \tag{2}$$

which belongs to both $L^\infty(\mathbb{R}^2)$ and $L^2(\mathbb{R}^2)$ due to boundedness and finite measure [8].

Proposition 1. *We now move to the functional-analytic framework by equipping $L^2(\mathbb{R}^2)$ with its standard inner product*

$$\langle f, g\rangle_{L^2} = \int_{\mathbb{R}^2} f(x)\,\overline{g(x)}\,dx, \tag{3}$$

which induces the Hilbert space norm $\|f\|_2 = \sqrt{\langle f, f\rangle}$ [14]. As a basic consequence, Parsevals identity asserts that $\|f\|_2^2 = \langle f, f\rangle$, ensuring consistency between the inner product and the norm.

Having established the Hilbert space setting, we introduce the central class of multiplication operators. *The first fundamental property of these operators is linearity. If $g \in L^\infty(\mathbb{R}^2)$ and $f, h \in L^2(\mathbb{R}^2)$, then [15]:*

$$M_g(\alpha f + \beta h) = \alpha M_g f + \beta M_g h,$$

with $(M_g f)(x) = g(x) f(x)$.

Theorem 1. *Beyond linearity, multiplication operators are also bounded. For $g \in L^\infty(\mathbb{R}^2)$, the operator norm of M_g satisfies*

$$\|M_g\| = \|g\|_\infty.$$

Indeed, for any $f \in L^2(\mathbb{R}^2)$,

$$\|M_g f\|_2^2 = \int_{\mathbb{R}^2} |g(x) f(x)|^2\,dx \le \|g\|_\infty^2 \int_{\mathbb{R}^2} |f(x)|^2\,dx = \|g\|_\infty^2 \|f\|_2^2.$$

Equality is attained (in the limit) for functions supported near points where $|g(x)|$ approaches $\|g\|_\infty$.

Lemma 1. *Specializing to indicator functions, multiplication by χ_i restricts the support of a function:*

$$\operatorname{supp}(M_{\chi_i} f) \subseteq S_i,$$

since $(M_{\chi_i} f)(x) = 0$ whenever $x \notin S_i$. Consequently, if S_i and S_j are disjoint, their indicator functions are orthogonal [4, 14, 15]:

$$\chi_i(x)\,\chi_j(x) = 0.$$

Lemma 2. *A crucial property of indicator functions is their idempotence:*

$$\chi_i(x)^2 = \chi_i(x), \qquad \forall x \in \mathbb{R}^2. \tag{4}$$

This observation generalizes to multiplication operators: if $g^2 = g$ almost everywhere, then $M_g^2 = M_g$.

The algebra of multiplication operators defined by pointwise products is straightforward: $M_f \circ M_g = M_{fg}$, and their adjoint is given by $M_g^* = M_{\overline{g}}$. When g is real-valued, the operator M_g is therefore self-adjoint [8].

Theorem 2. *Trace properties also play an important role. If g is integrable, then*

$$\mathrm{Tr}(M_g) = \int_{\mathbb{R}^2} g(x)\,dx. \tag{5}$$

In particular, for indicator functions χ_i, the trace reduces to the area A_i of the sector S_i. Furthermore, the trace enjoys the cyclic property $\mathrm{Tr}(AB) = \mathrm{Tr}(BA)$, whenever both products are trace-class [11].

The projection viewpoint yields additional inequalities. Any projection P satisfies

$$\|Pf\|_2 \le \|f\|_2, \qquad P^2 = P.$$

Projections corresponding to disjoint supports satisfy the orthogonality condition $PQ = 0$.

Moreover, if $g \ge 0$, then M_g is positive semidefinite since [8]:

$$\langle M_g f, f\rangle = \int_{\mathbb{R}^2} g(x)\,|f(x)|^2\,dx \ge 0, \qquad \text{if } g(x) \ge 0.$$

Proposition 2. *More generally, one has the operator inequality*

$$0 \le M_g \le \|g\|_\infty I,$$

which follows from boundedness and positivity [20].

Finally, classical inequalities from analysis underlie later operator estimates. The Cauchy–Schwarz inequality ensures

$$|\langle f, g\rangle| \le \|f\|_2\,\|g\|_2.$$

Theorem 3. ***(Youngs Inequality).*** *In scalar form, Youngs inequality states [19]:*

$$ab \le \frac{a^p}{p} + \frac{b^q}{q}, \qquad a,b \ge 0, \qquad \frac{1}{p} + \frac{1}{q} = 1. \tag{6}$$

Youngs inequality extends to integrals, asserting that for $f \in L^p$ and $g \in L^q$ one has [10]:

$$\int |f(x)g(x)|\,dx \le \|f\|_p\,\|g\|_q, \qquad \frac{1}{p} + \frac{1}{q} = 1.$$

The operator version of Youngs inequality generalizes the scalar case. For positive operators A, B and $p, q > 1$ with $\frac{1}{p} + \frac{1}{q} = 1$, one has [10]

$$AB \le \frac{1}{p}A^p + \frac{1}{q}B^q, \tag{7}$$

extending the classical bound to the noncommutative operator setting.

Theorem 4. ***(AM-HM Inequality).*** *Closely related to Youngs inequality is the inequality between the arithmetic mean (AM) and the harmonic mean (HM). For any $a, b > 0$ [5],*

$$\frac{a+b}{2} \ge \frac{2}{\frac{1}{a} + \frac{1}{b}}, \tag{8}$$

with equality if and only if $a = b$.

In general, for positive real numbers $a_1, \ldots, a_n$, the arithmetic and harmonic means are defined as

$$\mathrm{AM}(a_1, \ldots, a_n) = \frac{1}{n}\sum_{i=1}^{n} a_i, \qquad \mathrm{HM}(a_1, \ldots, a_n) = \frac{n}{\sum\limits_{i=1}^{n} a_i^{-1}},$$

and the inequality holds for all $n \ge 2$, with equality precisely when all a_i are equal. This inequality follows directly from the convexity of the reciprocal function $f(x) = \frac{1}{x}$, and it may be established through Jensens inequality or as a corollary of the AMGM inequality. It is particularly useful when dealing with reciprocal structures, and in our context, its role in the next part is to transform expressions involving sector parameters into more symmetric and tractable bounds, thereby aligning naturally with other classical inequalities such as AMGM and CauchySchwarz.

3 Main Results

In this section, we begin the development of our main contributions. The key object of study is the overlap of two measurable sectors $S_1, S_2 \subset \mathbb{R}^2$, which we represent using multiplication operators, projections, and their traces. The analysis builds systematically upon the results established in the preliminary concepts, which introduced indicator functions, properties of multiplication operators, the inner-product structure in L^2, and the relevant inequalities.

3.1 Overlap as Trace of Projection Product

Theorem 5. *Let $S_1, S_2 \subset \mathbb{R}^2$ be measurable sectors, and let χ_1, χ_2 denote their indicator functions as defined in 2. Let $P = M_{\chi_1}$ and $Q = M_{\chi_2}$ denote the multiplication operators associated with these indicator functions, as introduced in 3. Then the measure of the overlap of the two sectors satisfies*

$$A_{Overlap} = \int_{\mathbb{R}^2} \chi_1(x)\,\chi_2(x)\,dx = \langle \chi_1, \chi_2 \rangle_{L^2} = \mathrm{Tr}(PQ). \tag{9}$$

Proof. By definition (2.1), the indicator functions satisfy $\chi_i(x) \in \{0,1\}$ and are measurable. The overlap integral may be expressed as

$$\langle \chi_1, \chi_2 \rangle_{L^2} = \int_{\mathbb{R}^2} \chi_1(x)\,\chi_2(x)\,dx.$$

Next, by 4, multiplication operators compose as

$$(PQf)(x) = P(Qf)(x) = \chi_1(x)\big(\chi_2(x)f(x)\big) = (\chi_1(x)\chi_2(x))f(x),$$

which shows that $PQ = M_{\chi_1\chi_2}$.

Finally, by 5, the trace is given by

$$\mathrm{Tr}(PQ) = \int_{\mathbb{R}^2} \chi_1(x)\,\chi_2(x)\,dx = A_{\mathrm{Overlap}}.$$

Thus, we conclude that

$$A_{\mathrm{Overlap}} = \langle \chi_1, \chi_2 \rangle_{L^2} = \mathrm{Tr}(PQ).$$

□

3.2 Convex Young Inequality Bound

Theorem 6. *Define $p > 1$ and $q = \frac{p}{p-1}$ to be Hölder conjugates. Let $P = M_{\chi_1}$ and $Q = M_{\chi_2}$ be the multiplication operators corresponding to the indicator functions of sectors S_1 and S_2. Then the overlap satisfies the convex inequality bound:*

$$A_{Overlap} \leq \frac{1}{p}A_1 + \frac{1}{q}A_2,$$

where $A_i = \mathrm{Tr}(M_{\chi_i})$ is the area of sector S_i.

Proof. By 6, for $a, b \geq 0$ we have the Young inequality

$$ab \leq \frac{a^p}{p} + \frac{b^q}{q}.$$

Applying this pointwise to $a = \chi_1(x)$ and $b = \chi_2(x)$ yields

$$\chi_1(x)\chi_2(x) \leq \frac{\chi_1(x)^p}{p} + \frac{\chi_2(x)^q}{q}.$$

Since $\chi_i^p = \chi_i$ for indicator functions by 4, integrating both sides over $\mathbb{R}^2$ and using 5 gives

$$\int_{\mathbb{R}^2} \chi_1(x)\chi_2(x)\,dx \leq \frac{1}{p}\int_{\mathbb{R}^2} \chi_1(x)\,dx + \frac{1}{q}\int_{\mathbb{R}^2} \chi_2(x)\,dx.$$

Hence,

$$A_{\mathrm{Overlap}} \leq \frac{1}{p}A_1 + \frac{1}{q}A_2.$$

This establishes the desired inequality. □

Note: Throughout this paper, we have used the term nonlinear analytical model to describe our framework. It is important to note that the overlap functional in question is, mathematically, bilinear. However, we have employed this term to refer to the complex and unpredictable behavior of the system under study, rather than in its strict mathematical sense. The interaction between the overlap functional and other components of the model can lead to nonlinear behavior at a macro level.

3.3 Angular-Radial Geometric Bound (Restricted Domain Interpretation)

Theorem 7. *Let the restricted domain:*

$$\Omega_{Overlap} = \{r, \varphi : r < r_{\min},\ \varphi \in [\varphi_{start}, \varphi_{start} + \theta_{Overlap}]\}, \tag{10}$$

and let R be the restriction operator given by multiplication with the indicator function of $\Omega_{Overlap}$. The overlap satisfies:

$$A_{Overlap} \leq \langle R\chi_1, R\chi_2 \rangle \leq \tfrac{1}{2} r_{\min}^2 \theta_{Overlap}.$$

Proof. From 9 the overlap can be written as:

$$A_{\text{Overlap}} = \langle \chi_1, \chi_2 \rangle.$$

Restricting to the smaller domain Ω_{Overlap} gives:

$$A_{\text{Overlap}} \leq \langle R\chi_1, R\chi_2 \rangle.$$

Since outside Ω_{Overlap} the overlap is zero. Applying 1, the overlap is bounded above by the area of a sector of radius $r_{\min}$ and angle θ_{Overlap}, which yields:

$$A_{\text{Overlap}} \leq \tfrac{1}{2} r_{\min}^2 \theta_{\text{Overlap}}.$$

□

3.4 AngularAveraged Bound

Before stating the main theorem, we briefly explain the geometric and analytic intuition underlying the angular–averaged estimate. For circular sectors of equal radius, the overlap region is constrained primarily by the intersection of their angular supports, while the radial contribution is uniform across angles. From this perspective, it is natural to view each sector as distributing its area along its angular span, with an effective *angular density* given by the ratio A_i/θ_i, representing the area contributed per unit angle. When two sectors overlap over an angular interval of length θ_{Overlap}, the maximal possible contribution to the overlap area is governed by how much area each sector can supply within this common angular window. Rather than tracking exact geometric intersections, we average these angular densities and scale them by the size of the shared angular support. This averaging mechanism captures the idea that the overlap cannot exceed what is jointly available from both sectors per unit angle. The resulting bound therefore reflects a balance between angular extent and area distribution. The imposed monotonicity condition ensures that sectors with higher angular density are not paired with disproportionately smaller angular spans, preventing pathological configurations and allowing a symmetric and interpretable upper estimate. This viewpoint explains why the overlap area can be controlled by the average angular density multiplied by the common angular support.

Theorem 8. *Let S_1 and S_2 be two circular sectors of equal radius $r > 0$, having angular widths $\theta_1, \theta_2 \in (0, \pi]$. The corresponding areas of the sectors are given by:*

$$A_1 = \frac{1}{2} r^2 \theta_1, \qquad A_2 = \frac{1}{2} r^2 \theta_2.$$

Let $\Omega_{Overlap} \subseteq [0, \min(\theta_1, \theta_2)]$ represent the angular overlap, i.e., the angular length of the region common to both sectors in the polar coordinate system. We impose the following monotonicity matching condition:

$$\left(\frac{A_1}{\theta_1} - \frac{A_2}{\theta_2} \right) (\theta_1 - \theta_2) \geq 0.$$

This ensures that the angular density A_i/θ_i and the angular span θ_i vary in the same direction: if S_1 is denser (i.e., larger area per angle), then it must also have a wider angular spread, or vice versa. This condition avoids imbalanced configurations that could invalidate the inequality. Under this assumption, the area of the overlapping region satisfies the following bound:

$$A_{Overlap} \leq \theta_{Overlap} \cdot \frac{A_1 + A_2}{\theta_1 + \theta_2}. \tag{11}$$

Proof. Recall from 10 that R is the multiplication operator corresponding to the restricted domain

$$\Omega_{\text{Overlap}} = \{(r,\phi) : r < r_{\min},\, \phi \in [\phi_{\text{start}}, \phi_{\text{start}} + \theta_{\text{Overlap}}]\}.$$

R acts as a projection that "cuts down" both the radial and angular ranges of the sectors to the maximal region where overlap can occur. The trace of the composition is expressed as:

$$\text{Tr}(RP) = \int_{\mathbb{R}^2} (R\chi_1)(x)\, dx.$$

It is observed that $R\chi_1$ is nonzero only on the set $\Omega_{\text{Overlap}} \cap S_1$. Since the radial restriction $r < r_{\min}$ has already been enforced, the remaining restriction is purely angular. Consequently, the effect is determined by the fraction of the angular overlap:

$$\frac{\theta_{\text{Overlap}}}{\theta_1}. \tag{12}$$

Furthermore, according to 5 in Section 2 (trace of a multiplication operator), the trace of M_{χ_1} is given by the full area of the sector S_1:

$$\text{Tr}(M_{\chi_1}) = A_1.$$

By an identical line of reasoning, one has

$$\text{Tr}(RQ) = \int_{\mathbb{R}^2} (R\chi_2)(x)\, dx,$$

where the support of $R\chi_2$ lies only in $\Omega_{\text{Overlap}} \cap S_2$. The sector S_2 spans an angular interval of length θ_2, which is then cut down to θ_{Overlap} under the restriction. As a consequence, it is obtained that:

$$\text{Tr}(RQ) \le \frac{\theta_{\text{Overlap}}}{\theta_2} A_2.$$

From 7, the following inequality is satisfied:

$$\text{Tr}(PQ) \le \frac{1}{p}\text{Tr}(RP) + \frac{1}{q}\text{Tr}(RQ),$$

where $p, q > 1$ are Hölder conjugates. By substituting the bounds obtained in 11 and 12, the result becomes:

$$\text{Tr}(PQ) \le \frac{1}{p}\frac{\theta_{\text{Overlap}}}{\theta_1} A_1 + \frac{1}{q}\frac{\theta_{\text{Overlap}}}{\theta_2} A_2.$$

Since $1/p + 1/q = 1$, the common factor θ_{Overlap} can be factored out, and the inequality is rewritten as:

$$\text{Tr}(PQ) \le \theta_{\text{Overlap}} \left(\frac{A_1}{p\theta_1} + \frac{A_2}{q\theta_2} \right). \tag{13}$$

To prepare the ground for a more interpretable and symmetric estimate, we simplify the expression by selecting the arithmetic mean case of Hölder's inequality, namely $p = q = 2$, which eliminates the need for asymmetric weighting and leads to:

$$A_{\text{Overlap}} \le \frac{1}{2} \left(\frac{\theta_{\text{Overlap}}}{\theta_1} A_1 + \frac{\theta_{\text{Overlap}}}{\theta_2} A_2 \right).$$

The intermediate inequality can equivalently be expressed as:

$$A_{\text{Overlap}} \le \theta_{\text{Overlap}} \cdot \frac{1}{2} \left(\frac{A_1}{\theta_1} + \frac{A_2}{\theta_2} \right). \tag{14}$$

Here, each term A_i/θ_i represents the angular density of the sector S_i, i.e., its area per unit angle. To further symmetrize the expression, we invoke the arithmetic–harmonic mean inequality. Under the monotonicity condition

$$\left(\frac{A_1}{\theta_1} - \frac{A_2}{\theta_2} \right) (\theta_2 - \theta_1) \ge 0,$$

we have:

$$\frac{1}{2} \left(\frac{A_1}{\theta_1} + \frac{A_2}{\theta_2} \right) \ge \frac{A_1 + A_2}{\theta_1 + \theta_2}.$$

Consequently, we arrive at the bound

$$A_{\text{Overlap}} \le \theta_{\text{Overlap}} \cdot \frac{A_1 + A_2}{\theta_1 + \theta_2},$$

which completes the proof. □

For clarity , we explicitly state the following:

- Young's inequality version: The operator version of Youngs inequality (Equation (7)) is used (See [10]).
- No commutativity assumption: The present analysis does not require the assumption of operator commutativity.
- Operator properties: All operators used in this analysis are positive and trace-class, and these properties are fully explained in the relevant sections.

The result established in Theorem 8 differs fundamentally from classical geometric formulas that aim at computing the exact area of intersection. In the existing literature, the overlap of circular or sectorial regions is typically analyzed through explicit geometric constructions, involving the determination of intersection points, arc equations, and case–dependent configurations. As a consequence, such methods are highly sensitive to the relative positions and orientations of the sectors and do not readily yield uniform analytic estimates. In contrast, the angular–averaged bound derived in Theorem 8 provides a configuration–independent analytic upper bound that depends only on global sector parameters, namely the sector areas and their angular widths. By avoiding explicit computation of geometric intersections, the proposed bound offers a simpler and more robust alternative when exact formulas are either unavailable or unnecessary. It should be emphasized that, unlike classical geometric approaches, the result of Theorem 8 is not intended to produce the exact overlap area and may be loose for certain configurations. Its main advantage lies in delivering a guaranteed and interpretable analytic estimate, which complements previous geometric methods and is particularly useful for theoretical analysis and algorithmic applications.
The following example illustrates the applicability of the angular–averaged bound derived in Theorem 8.

Example 1. (**Angular Overlap of Two Circular Sectors:**) Consider two circular sectors S_1 and S_2 with equal radii $r = 2$. The angular span of S_1 is $\theta_1 = \pi/2$ (90ř), and that of S_2 is $\theta_2 = \pi/3$ (60ř). The centers of the sectors are located at $(0,0)$ and $(1.5,0)$, respectively. The initial direction of S_1 is 30°, while S_2 begins at 60°.

To determine the angular overlap θ_{Overlap}, we consider the angular intervals:

$$S_1 : [\theta_1^{\text{start}}, \theta_1^{\text{end}}] = [\pi/6, 2\pi/3], \qquad S_2 : [\theta_2^{\text{start}}, \theta_2^{\text{end}}] = [\pi/3, 2\pi/3].$$

The intersection interval is:

$$\theta_{\text{Overlap}} = [\max(\pi/6, \pi/3), \min(2\pi/3, 2\pi/3)] = [\pi/3, 2\pi/3] \Rightarrow \theta_{\text{Overlap}} = \pi/3.$$

The area of each sector is computed via the standard formula:

$$A_1 = \frac{1}{2} r^2 \theta_1 = \frac{1}{2} \cdot 4 \cdot \frac{\pi}{2} = \pi, \qquad A_2 = \frac{1}{2} r^2 \theta_2 = \frac{1}{2} \cdot 4 \cdot \frac{\pi}{3} = \frac{2\pi}{3}.$$

Applying the angular overlap bound (Equation (50)):

$$A_{\text{Overlap}} \leq \theta_{\text{Overlap}} \cdot \frac{A_1 + A_2}{\theta_1 + \theta_2} = \frac{\pi}{3} \cdot \frac{\pi + 2\pi/3}{\pi/2 + \pi/3} = \frac{2\pi}{3} \approx 2.0944.$$

To verify the validity of the angular overlap bound stated in Theorem 4 for the constructed example, we proceed by carefully examining the geometric configuration and checking that all necessary assumptions for the theorem are satisfied. In this scenario, the two circular sectors are characterized by angular spans $\theta_1 = \pi/2$ and $\theta_2 = \pi/3$, corresponding to sectors S_1 and S_2 respectively.

Both sectors are constructed with radius $r = 2$ and have angular spans $\theta_1 = \pi/2$ and $\theta_2 = \pi/3$, respectively. The area of each sector is:

$$A_1 = \frac{1}{2} r^2 \theta_1 = \pi, \qquad A_2 = \frac{1}{2} r^2 \theta_2 = \frac{2\pi}{3}.$$

The angular densities of the two sectors, defined as A_i/θ_i, quantify the area per unit angle for each sector. Substituting the expressions above, we see that both sectors have equal angular densities:

$$\frac{A_1}{\theta_1} = \frac{\pi}{\pi/2} = 2, \qquad \frac{A_2}{\theta_2} = \frac{2\pi/3}{\pi/3} = 2.$$

This equality directly satisfies the monotonicity matching condition required for the bound to hold:

$$\left(\frac{A_1}{\theta_1} - \frac{A_2}{\theta_2}\right)(\theta_1 - \theta_2) \geq 0,$$

which evaluates to zero in this case. Hence, the condition is satisfied trivially, ensuring the validity of the bound.

In addition to the theoretical verification, Figure 1 provides a visual representation of the sectors S_1 and S_2 placed with partial angular overlap.

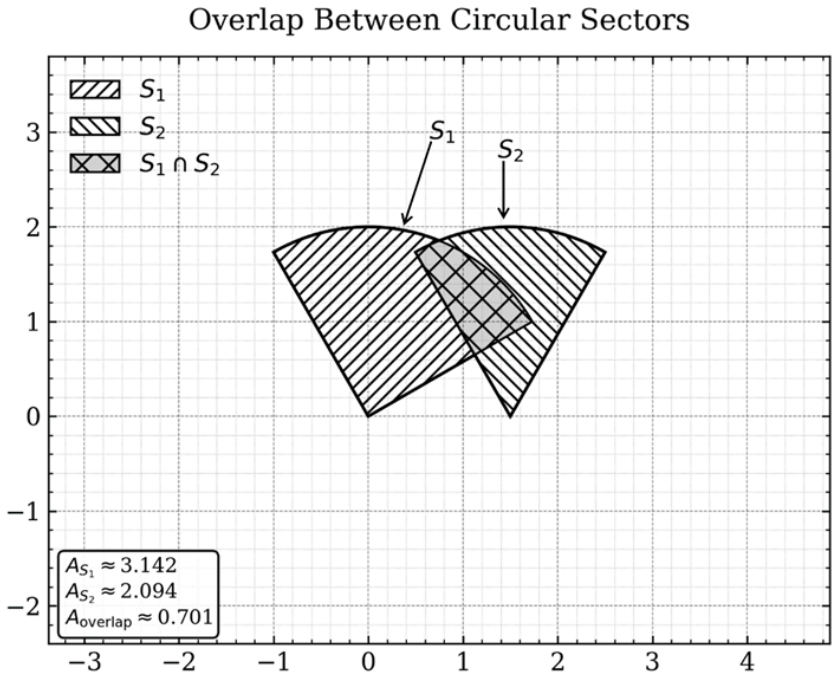

Figure 1. Consider the overlap between two circular sectors S_1 and S_2 with angular spans $\theta_1 = \frac{\pi}{2}$ and $\theta_2 = \frac{\pi}{3}$, sharing an intersection angle $\theta_{\text{Overlap}} = \frac{\pi}{3}$. The numerically computed overlap area is $A_{\text{Overlap}} \approx 0.701$, which satisfies the theoretical upper bound given by

$$A_{\text{Overlap}} \leq \theta_{\text{Overlap}} \cdot \frac{A_1 + A_2}{\theta_1 + \theta_2} = \frac{2\pi}{3} \approx 2.0944.$$

The configuration clearly shows the overlapping region, shaded in gray. A numerical simulation using polygonal approximation confirms that the actual intersection area is

$$A_{\text{Overlap}} \approx 0.701,$$

while the theoretical bound predicted by the inequality is

$$A_{\text{Overlap}} \leq \theta_{\text{Overlap}} \cdot \frac{A_1 + A_2}{\theta_1 + \theta_2} = \frac{\pi}{3} \cdot \frac{\pi + 2\pi/3}{\pi/2 + \pi/3} = \frac{2\pi}{3} \approx 2.0944.$$

This demonstrates that the observed value lies strictly below the theoretical upper limit. It confirms that the derived inequality is not only mathematically valid under the assumed conditions, but also practically sharp, with the simulated data falling well within the predicted bound.

4 Conclusion

In this work, we presented an operator–theoretic framework for analyzing the overlap of circular sectors, reformulating the overlap area as a trace of multiplication operators on $L^2(\mathbb{R}^2)$. This perspective allowed us to move beyond purely geometric constructions and to

systematically derive explicit upper bounds using classical functional inequalities. A key outcome of the proposed approach is the angular–averaged bound, which controls the overlap area in terms of the common angular support and the average angular densities of the sectors. This bound is symmetric, interpretable, and computable, and does not require explicit determination of geometric intersection points. As such, it provides a robust alternative to exact but configuration–dependent geometric formulas. Beyond the specific results obtained, the operator–based viewpoint introduced in this paper establishes a conceptual bridge between planar geometry and functional analysis. This framework opens several directions for future research, including extensions to higher–dimensional settings, randomized angular configurations, and efficient computational schemes for real–time overlap estimation in applied problems.

Authors' Contributions

The authors declare that they have no known competing financial interests or personal relationships that could have appeared to influence the work reported in this paper.

Data Availability

All data in the paper are available from the corresponding authors upon reasonable request.

Conflicts of Interest

The authors declare that there is no conflict of interest.

Ethical Considerations

The authors have diligently addressed ethical concerns, such as informed consent, plagiarism, data fabrication, misconduct, falsification, double publication, redundancy, submission, and other related matters.

Funding

This research did not receive any grant from funding agencies in the public, commercial, or nonprofit sectors.

References

[1] G. Andrea, Wireless Communications, 1st ed., Cambridge University Press, Cambridge, UK, 35–65, (2005).

[2] R. Courant, and H. Robbins, What is Mathematics?, 2nd ed., Oxford University Press, Oxford, UK, 180–182, (1996).

[3] H. Federer, Geometric Measure Theory, Springer, Berlin, 275–280, (1969).

[4] G.B. Folland, Real Analysis: Modern Techniques and Their Applications, 2nd ed., Wiley, New York, 254–255, (1999).

[5] K. Gaitanas, A New Proof of the AM-GM-HM Inequality, 1–3, (2020).

[6] M. Garcia, and A. Patel, Novel Techniques for Overlap Estimations in Circular Configurations, (2023).

[7] P. Glasserman, Monte Carlo Methods in Financial Engineering, 1st ed., Vol. 53, Springer, New York, 1–20, (2003).

[8] J.K. Hunter, Measure Theory, Department of Mathematics, University of California at Davis, Davis, California, (2011).

[9] R. Johnson, and L. Chen, Advancements in Nonlinear Analysis for Geometric Applications, Journal of Nonlinear Mathematics, 45(2), 145–160, (2023).

[10] T. Kosem, Matrix Versions of Youngs Inequality, Mathematical Inequalities & Applications Journal, Vol. 12, Zagreb, Croatia, 242–249, (2009).

[11] E. Kowalski, Spectral Theory in Hilbert Spaces, ETH Zürich, Zürich, Switzerland, (2009).

[12] A. Kumar, and S. Ghosh, Nonlinear Intersections in Geometric Measure Theory, Journal of Mathematical Analysis, 35(4), 450–465, (2021).

[13] T. Mendez, and S. Kim, Operator Inequalities in Circular Geometry, International Journal of Functional Analysis, 58(1), 75–89, (2024).

[14] J. Miller, Probability and Measure, University of Cambridge, Cambridge, UK, (2016).

[15] L. Nguyen, H. Priestley, and G. Seregin, Functional Analysis II, University of Oxford, Mathematical Institute, Oxford, UK, (2018).

[16] J. O'Rourke, Computational Geometry in C, 2nd ed., Cambridge University Press, Cambridge, UK, 227–250, (1998).

[17] R. Patel, and S. Kumar, Recent Advances in Circular Geometry Analysis, Journal of Geometric Analysis, 29, (2020).

[18] B. Simon, Trace Ideals and Their Applications, 2nd ed., American Mathematical Society, Providence, RI, (2010).

[19] J.M. Steele, The CauchySchwarz Master Class: An Introduction to the Art of Mathematical Inequalities, 1st ed., Cambridge University Press, Cambridge, UK, 1–10, (2004).

[20] J. Voigt, The essential norm of multiplication operators on $L^p(\mu)$, arXiv, 1–2, (2022).